KINETIC AND ENERGETIC MODEL FOR THE PRIMARY PROCESSES IN PHOTOSYSTEM II

GÜNTHER H. SCHATZ, HELMUT BROCK, AND ALFRED R. HOLZWARTH
Max-Planck-Institut für Strahlenchemie, D-4330 Mülheim a. d. Ruhr, Federal Republic of Germany

ABSTRACT A detailed model for the kinetics and energetics of the exciton trapping, charge separation, charge recombination, and charge stabilization processes in photosystem (PS) II is presented. The rate constants describing these processes in open and closed reaction centers (RC) are calculated on the basis of picosecond data (Schatz, G. H., H. Brock, and A. R. Holzwarth. 1987. *Proc. Natl. Acad. Sci. USA.* 84:8414–8418) obtained for oxygen-evolving PS II particles from *Synechococcus sp.* with ~80 chlorophylls/P_{680}. The analysis gives the following results. (*a*) The PS II reaction center donor chlorophyll P_{680} constitutes a shallow trap, and charge separation is overall trap limited. (*b*) The rate constant of charge separation drops by a factor of ~6 when going from open (Q-oxidized) to closed (Q-reduced) reaction centers. Thus the redox state of Q controls the yield of radical pair formation and the exciton lifetime in the Chl antenna. (*c*) The intrinsic rate constant of charge separation in open PS II reaction centers is calculated to be ~2.7 ps^{-1}. (*d*) In particles with open RC the charge separation step is exergonic with a decrease in standard free energy of ~38 meV. (*e*) In particles with closed RC the radical pair formation is endergonic by ~12 meV. We conclude on the basis of these results that the long-lived (nanoseconds) fluorescence generally observed with closed PS II reaction centers is prompt fluorescence and that the amount of primary radical pair formation is decreased significantly upon closing of the RC.

INTRODUCTION

The primary processes of excitation trapping, charge separation, and charge stabilization in photosystem II (PS II) are still much less studied than those in bacterial reaction centers (RCs).[1] It has been agreed that the nature of the primary (intermediate) electron acceptor I is pheophytin *a* (1–3). However, it is poorly understood whether the radical pair is also formed in RCs in which the first quinone acceptor Q is reduced (closed RC). Early experiments with PS II particles have suggested efficient charge separation and consecutive charge recombination with a time constant of ~2–4 ns under such conditions (4). The same point of view was taken in reference 2. The results of the analysis of chlorophyll (Chl) fluorescence decay data (5) and of time-resolved photovoltage measurements (6) have led to conclusions that were in conflict with the above-mentioned studies. The model proposed in reference 5 suggested a strongly decreased yield of radical pair formation and an increase in the yield of prompt fluorescence emission upon reducing the first quinone acceptor (closed RC) of PS II. Recently, we have reported on correlated picosecond absorbance and fluorescence measurements using isolated oxygen-evolving PS II particles from the thermophilic cyanobacterium *Synechococcus sp.* and low-intensity picosecond laser spectroscopy (3, 7). The data were interpreted qualitatively in terms of a model which assumes that the reaction center of PS II constitutes a shallow trap for an exciton which is delocalized over the complete chlorophyll antenna system. We now describe the kinetic model in detail by solving the corresponding rate equations and use the solutions for a quantitative analysis of the experimental data described earlier (3). From this analysis we obtain the complete set of rate constants in this model describing the steps of exciton trapping from the excited antenna as well as the charge separation, charge stabilization, and charge recombination processes in the RCs. By comparing the kinetic data from both open (Q-oxidized) and closed (Q-reduced) RCs new insights are gained with respect to the effects of the reduction of Q on the primary processes. It will be shown that the redox state of Q determines the rate constant and quantum yield of the primary radical pair formation. The thermodynamic and mechanistic implications of this regulative control by the quinone acceptor are discussed. Our results indicate a reduced probability for formation of the primary radical pair in closed RCs as compared with open RCs.

RESULTS

Kinetic Model

The kinetic model suitable to describe the experimental data from reference 3 is presented in Fig. 1. It comprises in

These results have been presented in part at the Deutsche Physikertagung, Berlin, March 1987.

[1] *Abbreviations used in this paper:* Chl, chlorophyll; I, primary electron acceptor (pheophytin); P and P_{680}, reaction center donor chlorophyll of PS II; PS, photosystem; Q, primary quinone acceptor; RC, reaction center; SSTT, single-step transfer time.

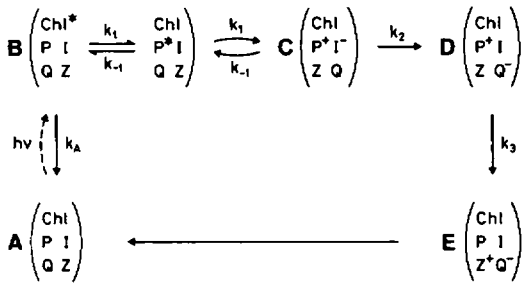

FIGURE 1. Kinetic model of the primary reactions in open PS II. In this scheme the rate constants k_j describe $k_A = k_d + k_{rad}$, the radiationless plus the radiative decay of Chl*; k_1 and k_{-1}, the processes of entering and leaving the trap (often called trapping and detrapping); k_1, the apparent primary charge separation; k_{-1}, charge recombination to the excited state; k_2 and k_3, the process of charge stabilization associated with the relaxation of I^- and P^+ rereduction, respectively. For closed PS II the rate constant k_2 is replaced by k_2' (cf. also Table II) leading to as yet unspecified product(s) instead of D.

the form of a matrix all components which are known to be involved in the primary processes. The ground state is represented by state A; the states reached after charge separation and charge stabilization steps are represented by the states C, D, and E, respectively. The excited states are represented by a generalized state B (see Fig. 1). Such a model is based on the assumption that a tight coupling and thus a very fast and reversible excitation transfer is realized between all antenna chlorophylls and the reaction center donor chlorophyll, P. This fast equilibrium is assumed to be established on a time scale comparable with or shorter than the time resolution in our experiment (3), i.e., within a couple of picoseconds. In this case, the equilibration

$$\mathrm{Chl^*\ P} \underset{k_{-1}}{\overset{k_1}{\rightleftharpoons}} \mathrm{Chl\ P^*}$$

would not be experimentally resolved and the overall decay of an equilibrated excited state would be limited by the rate of primary charge separation $P^*\ I \rightarrow P^+\ I^-$. This feature is typical for the so-called trap limit of the exciton decay (8, 9). Another feature of our kinetic scheme (Fig. 1) is the reversible energy partition between the excited states (state B) and the radical pair (state C). Both of these features of our model are consistent with experimental observations, as will be shown in the Discussion.

Quantitative Kinetic Analysis

The differential equations describing the scheme given in Fig. 1 are solved by application of the Laplace transform method as shown in the Appendix. Briefly, the results of Eq. A13–A15 show that the kinetics of Chl* and of the pheophytin anion (I^-) are biexponential (with lifetimes τ_1 and τ_2). The kinetics of P^+ is characterized by three exponentials with lifetimes τ_1, τ_2, and τ_3. The lifetime τ_3 simply equals $1/k_3$ (Eq. A4) because the corresponding process consists solely in the reduction of P^+ (see Eq. A15). The other two lifetimes (τ_1 and τ_2) are functions of all the rate constants k_A, k_1, k_{-1}, and k_2 (see Eqs. A2 and A3).

The amplitude factors (equal to normalized concentrations) by which the various pigments, i.e., Chl*, I^-, and P^+, contribute to the different kinetic phases are solely functions of all rate constants k_j (see Eqs. A13–A15) and the initial conditions (only Chl* excited). Hence, the unknown rate constants k_1, k_{-1}, k_2, and k_A can be determined from experimental data on four linearly independent parameters. Three of these parameters are chosen to be τ_1, τ_2, $^{Chl}a_1$ (or $^{Chl}a_2$), i.e., the lifetimes and relative amplitude factors describing the decay of Chl*. As the fourth parameter we use $^Pa_3$ (c.f. Appendix), which is identical to the absolute quantum yield of charge separation (Z^+PIQ^- formation). Alternatively we could assume a value for k_A and then calculate $^Pa_3$. The lifetimes and amplitudes of Chl* were measured in reference 3. Their values as recalled in Table I are obtained from the original fluorescence decay data after correcting for the presence of a long-lived component which was most likely due to an allophycocyanin contamination (see detailed discussion in reference 3).

The quantum yield of charge stabilization in PS II (at the state $Z^+\ PIQ^-$) is usually assumed to be in the range of 0.65 to 0.95 (10–12). Using a value of $^Pa_3 = 0.85$ for open PS II we calculate from our data the values of the rate constants k_j as given in Table II. Increasing the value of $^Pa_3$ to a maximum of 0.93 (as suggested in reference 11) has primarily the effect of decreasing the value of k_A (to 0.55 ns^{-1}) but has only a small effect (<6%) on the other rate constants. An analogous procedure can be applied to closed PS II. In that case any long-lived product of a forward reaction from $P^+I^-Q^-$ is assumed to be formed with a yield of $^Pa_3 \leq 0.15$. This value corresponds to the approximate detection limit of our absorbance change measurements (3), above which a bleaching due to a long-lived species (e.g., Chl- or P-triplet [13] or a stabilized radical pair [14]) would have been detected. It also corresponds to the results of direct measurements of triplet formation in chloroplasts (11). Changing the value of $^Pa_3$ in closed RCs results in an almost proportional change of k_2' and has only a small effect on the other rate constants. (Note that in closed RCs, k_2' replaces the rate constant k_2 for open RCs,

TABLE I
LIFETIMES τ_i AND RELATIVE AMPLITUDES OF CHLOROPHYLL FLUORESCENCE DECAYS

i	F_o		F_{max}	
	ps	%	*ps*	%
1	80	(78)*	220	(48)
2	520	(22)	1,300	(52)

Obtained from measurements reported in reference 3 using PS II particles with ~80 Chl/P_{680} under conditions for F_o (open centers) and F_{max} (closed centers), respectively. A third component of low amplitude due to an impurity has been omitted (see text).
*Relative amplitudes in parentheses.

TABLE II
RATE CONSTANTS k_j (ns^{-1}) ACCORDING TO THE KINETIC SCHEME IN FIG. 1

	Open	Closed	Open/closed ratio
k_A	0.9	1.1	0.8
k_1	9.3	1.5	6.2
k_{-1}	2	2.4	0.8
k_2	2	—	—
k_2'	—	0.3	—
${}^{P}a_3$	0.85	0.15	—

Calculated as described in text using the results of fluorescence kinetics for open and closed RCs of PS II (Table I) and the assumed values of ${}^{P}a_3$. Estimated error, ±15%.

and now describes alternative forward reactions other than charge stabilization as, e.g., formation of a triplet and/or of a relaxed radical pair state.)

The rate constants k_j (c.f. Fig. 1 and Table II) as calculated from the results of picosecond experiments (3) for open and closed RCs reveal a couple of interesting effects. The rate constant k_A changes only to a minor extent, i.e., the reduction of Q has, if any, only a minor effect on the intrinsic (radiative and radiationless) deactivation processes of antenna Chl*. The value calculated here suggests that the antenna complex uncoupled from the RC would show a fluorescence lifetime of ~1 ns. Indeed, similar values (1.1–1.2 ns) are observed in aggregates of isolated light-harvesting Chl *a*/*b* complexes (15–17). The electron transfer step $I^-Q \rightarrow I\,Q^-$ is characterized by a time constant ($1/k_2$) of 450 ps in open RCs. The latter process vanishes upon reduction of Q. The significant decrease from k_2 to k_2' upon closing the RC correlates with the finding of an insignificant triplet yield under our conditions. However, the possibility is not excluded that with excitation pulses of higher photon densities the triplet yield may be increased due to singlet–singlet annihilation, and triplets may be observable as absorbance changes in the nanosecond time range. This mechanism may be the origin of the third, long-lived component reported in reference 7 with closed RCs excited with higher photon fluences. The most striking change upon closing the RCs consists in the reduction of the rate constant k_1 of charge separation by a factor of ~6 as compared with open RCs. This reduction shows that the primary charge separation process strongly depends on the redox state of Q. After reduction of Q the primary radical pair formation is much slower and occurs with strongly reduced efficiency. Since the value of k_{-1} increases only slightly when going from open to closed RCs, the ratio k_1/k_{-1} drops by a factor of 7.5 (from 4.6 to ~0.6) upon Q reduction. This drop indicates that the equilibrium (Chl* P I) ⇌ (Chl P^+I^-) is shifted drastically to the side of the excited state of the antenna chlorophylls. Consequently the lifetime of Chl* and thus the yield of Chl* fluorescence is enhanced, whereas the yield of P^+I^- formation is decreased upon reduction of Q. This influence of Q reduction on the yield of P^+I^- formation is in contrast to the hypothesis put forward by Klimov et al. (4).

The amplitude factors by which the various pigments contribute to the different kinetic phases are given in Table III. In the first row, the two amplitude factors of Chl* decay are noted. The second row shows the amplitude factors for the rise and decay, respectively, of the pheophytin anion as intermediate electron acceptor. Its value can be taken as a measure of primary radical pair formation (see Discussion). Evidently, much less reduced pheophytin is formed in closed as compared to open reaction centers. This finding reflects the change in the ratio k_1/k_{-1} already mentioned. The third row gives the rise and decay contributions by P^+. From these amplitude factors the time dependence of the yield or relative concentration of the respective pigment component can be calculated.

The columns in Table III represent the composite character of the absorbance difference spectra associated with the respective lifetime τ_i. These difference spectra were given in reference 3. The difference spectra describing trapping and primary charge separation, associated with τ_1, obviously contain similar (but not equal) contributions from the absorption difference spectra of all three pigment components. In the case of open RCs the spectrum of lifetime component τ_2 contains a dominant contribution by the pheophytin-anion and small ones by Chl* and P^+. With closed RCs the lifetime component τ_2 is dominated by the decay of excited antenna chlorophyll, Chl*. Only the process giving rise to component τ_3 in open centers yields a pure absorbance difference spectrum of a single pigment species, i.e., the P^+/P difference spectrum due to P^+ reduction. This follows from Eq. A16.

DISCUSSION

In any complex reaction scheme with reversible, branched, and consecutive reactions, it is generally not possible to

TABLE III
AMPLITUDE FACTORS ACCORDING TO EQS. A13–A15 DESCRIBING NORMALIZED CONTRIBUTIONS OF ANTENNA CHLOROPHYLL (Chl), PHEOPHYTIN (I), AND P_{680} (P) TO THE OBSERVED KINETIC COMPONENTS OF PS II

RC state:	Open			Closed		
Lifetime index *i*:	1	2	3	1	2	3
Pigment component						
${}^{Chl}a_i$	0.78	0.22	—	0.48	0.52	—
${}^{I}a_i$	−0.87	0.87	—	−0.39	0.39	—
${}^{P}a_i$	−0.72	−0.13	0.85	−0.36	0.21	0.15*

Data have been calculated from the set of parameters given in Table II. A positive value denotes a decay term, a negative value a rise term.
*Maximal relative concentration of long-lived components in closed RC, which was estimated to remain unresolved as separate kinetic component under the experimental conditions in reference 3.

extract information on rate constants without a formal kinetic analysis. We have presented the analytical solution to the rate equations of a kinetic scheme as shown in Fig. 1. In this way the complete set of rate constants is obtained from the experimental data (3) without any further assumptions rather than being based on (*a*) the validity of the kinetic scheme itself and (*b*) the value of product yield, ${}^{P}a_3$. The scheme is based on the same principles as our former model (5) which was developed to describe fluorescence kinetics only. It is now extended by an additional state (state E in Fig. 1) to describe the absorbance changes by P^+ as well. This scheme comprises the scheme of minimal complexity required to allow the interpretation of the present experimental data.

According to our kinetic scheme (see Fig. 1), the state B is a generalized excited state of any chlorophyll species, including all the antenna Chl* as well as P*. Hence, k_1 is the apparent rate constant of charge separation. It is different from the intrinsic rate constant, k_1^{int} by the factor of partition of the exciton between P and all Chl molecules in the core antenna. According to the scheme

$$(\text{Chl}^* \cdot \text{P}) \underset{k_{-t}}{\overset{k_t}{\rightleftharpoons}} (\text{Chl} \cdot \text{P}^*),$$

this partitioning can be described by the rate constants k_t and k_{-t} of entering and leaving the trap, respectively, and the degree of degeneracy of the state (Chl* · P). In a simple model this degeneracy is N-fold if N is the number of equivalent antenna Chl molecules coupled to P. Then, the apparent rate constant relates to the intrinsic one according to

$$k_1^{int} = k_1 \cdot N \frac{k_{-t}}{k_t}. \qquad (1)$$

This equation is identical with that derived by Pearlstein for the trap limit (8, 18) if extrapolated to large values of N.

The ratio k_{-t}/k_t may be described by the Boltzmann distribution

$$\frac{k_{-t}}{k_t} = \frac{[\text{Chl}^* \cdot \text{P}]}{[\text{Chl} \cdot \text{P}^*]} = \exp\left[-hc/kT(\lambda_{\text{Chl}}^{-1} - \lambda_{\text{P}}^{-1})\right], \qquad (2)$$

using the wavelengths of maximum absorbance of antenna Chl and P, λ_{Chl} and λ_P, respectively. In our PS II particles the maximum absorption in the red is at $\lambda_{Chl} = 673$ nm. The maximum absorbance of P is assumed to be at 680 nm. With these values and a value of N of ~80 (19), one calculates from Eqs. 1 and 2 an intrinsic rate constant of ~370 ns^{-1} (according to $k_1^{int} = 9.3\ ns^{-1} \cdot 80 \cdot 1/2$) corresponding to a time constant of ~2.7 ps. Interestingly, this is very close to the value of 2.8 ps which was measured directly for the primary charge separation in isolated bacterial reaction centers devoid of any antenna pigments (20–23).

It is interesting at this stage to make a comparison with the theoretical model put forward by Pearlstein (8) and experimental data related to that model. Values for the single-step energy transfer times (SSTT) between neighboring antenna chlorophylls are suggested to be in the range of 50 (24) to 200 fs (25). In a simple cubic lattice of 80 Chl molecules, an exciton will visit the trap P in average after 121 single steps of random walk (8). These data therefore correspond to first passage times of 6 and 24 ps, respectively. Thus, the number of visits at P before radical pair formation is calculated to be in the range of 3.3 to 13.3 using the SSTT values of 200 or 50 fs, respectively, and the exciton lifetime of 80 ps. For some other types of lattice even larger numbers of visits are calculated. Therefore, it appears that the exciton decay kinetics in a complete photosystem II complex (i.e., RC plus antenna) are clearly limited by the relatively slow step of charge separation. This situation is termed the trap-limited case (8, 26), in which the exciton kinetics can be described by random walk models (9, 24, 26). In the trap-limited case the exciton lifetime depends linearly on the number of pigment molecules in the antenna domain (18, 26). Therefore, a linear correlation of the trapping kinetics with the antenna size of PS II is expected. Such a correlation is indicated by experimental observations. In PS II particles with ~80 Chl/P_{680} the fast component of Chl* kinetics has a time constant of 80 ps (3), whereas in unfractionated thylakoids with typically 200–250 Chl/P_{680} (27) the corresponding time constant is 250–300 ps (28, 29).

Notably, a similar behavior is observed with other photosystems. Charge separation in isolated bacterial RC with Q oxidized is characterized by lifetimes in the range of 2.8 (20–23) to ~4 ps (30). The intact chromatophores show short-lived excited-state lifetimes of BChl of typically 50–70 ps (31–33) with antenna sizes of ~30–50 BChl/RC. Furthermore charge separation may occur with a time constant of 2.8 ps also in the reaction center of photosystem I. This time was estimated from fluorescence lifetime measurements in dependence on the antenna size (25) using model assumptions from references 26 and 34. It should be noted that the latter approaches are based on molecular parameters such as Förster transfer rate constants and the type of lattice mimicking the pigment organization. These details are essential in the theories developed by Pearlstein (26) and Shipman (34). In contrast, our basic kinetic model is not dependent on such molecular parameters but rather on ensemble kinetic data. Hence, it is insensitive to, for example, the question of whether P_{680} is a monomeric or dimeric special chlorophyll.

Our model generally implies that both the exciton coupling between the chlorophyll pigments in a photosystem and the exciton–phonon coupling are strong enough to achieve both randomization of the excited state and thermal equilibrium with the lattice, respectively, within the exciton lifetime. The intermolecular exciton coupling energy V between antenna chlorophylls may be ~100 cm^{-1}

(=12.4 meV), i.e., in the order of or somewhat lower than the spectral band width to match the dipole–dipole interaction in a crystallike lattice as proposed in reference 24. Such an interaction energy corresponds (according to $t \sim h/2\pi V$) to a SSTT of ~50 fs. The exciton-phonon coupling energy may be in the order of 1 cm^{-1} (35 and references therein) corresponding to a time of ~5 ps after which thermal equilibrium with the lattice is expected. Hence, within such a model thermal equilibrium between Chl*, P*, and the lattice would be reached if the overall exciton lifetime is significantly longer than 5 ps, i.e., if the antenna size is relatively large. In contrast, no thermal equilibrium might be reached in isolated RC complexes devoid of antenna pigments.

So far we have analyzed our data on the basis of the model shown in Fig. 1 and on this basis have arrived at detailed conclusions. We have also presented in detail the assumptions underlying this model. It remains to be shown that this model is (*a*) in agreement with experimental observations and that (*b*) it is capable of making physically reasonable predictions.

In our view the following experimental observations support, inter alia, the validity of our kinetic reaction scheme. (*a*) A drastic increase is observed in the time constant of the fastest fluorescence decay component when RCs were closed. This indicates that a diffusion-limited exciton kinetics is unlikely, since the exciton diffusion should not be influenced by the redox state of Q. (*b*) The obvious proportionality between the time constant of trapping and the antenna size mentioned above indicates a tight exciton coupling and a fast equilibration between all PS II–antenna chlorophylls. This proportionality seems to hold also for other types of reaction center/antenna complexes. (*c*) The time constant of charge stabilization of ~500 ps observed in absorption as the reoxidation of the pheophytin anion is also found in the fluorescence decay kinetics of open RCs (3). This necessarily indicates that an exciton visits P several times before being trapped by photochemistry. (*d*) Recently it was proposed (36) that in the case of exciton–phonon interaction being much smaller as compared with exciton–exciton interaction (which is assumed to be the case in Chl antennae) the exciton motion may be coherent for times up to a few picoseconds. This would also favor a trap-limited exciton decay kinetics.

The control of the yield and rate of P^+I^- formation by the redox state of Q is considered to be a consequence of the electrical field created by the negative charge on Q^- and the smaller distance between Q^- and I than from Q^- to P. This electrical field increases the energy content of the electrical dipole of P^+I^-. A calculation based on the Coulomb potential of point charges on P, I, and Q in a homogeneous dielectric with $\epsilon_r = 4.5$ (corresponding to a typical transmembrane capacitance of 1 $\mu F/cm^2$ [37] and a membrane normale of 4 nm) for the distances $\overline{PI}$ = 13.5 Å, $\overline{IQ}$ = 17 Å, and $\overline{PQ}$ = 27 Å (assumed in approximate analogy to data from bacterial RCs [38]) yields an energy increase in the order of 120 meV. As argued above, one may apply equilibrium thermodynamics to describe the energy partition between excited and charged states in RCs if the exciton lifetimes are much longer than the time for exciton-lattice relaxation. This requirement is presumably fulfilled with PS II particles. Thus, the standard free energy difference between the radical pair states P^+I^-Q or $P^+I^-Q^-$ on the one hand and the corresponding excited states on the other hand can be calculated according to $\Delta G = -kT\,ln\,(k_1/k_{-1})$. Using the data from Table II the following results are obtained for the PS II particle with 80 Chl/P_{680}. (*a*) Charge separation in open RCs is exergonic and associated with a decrease in standard free energy of 38 meV. (*b*) In closed RCs charge separation is endergonic affording a standard free energy increase of 12 meV. This is schematically shown in Fig. 2, referring to $[P(Chl_{80})]^*$ as the excited states from which fluorescence is observed. These excited states are placed on different standard free energy levels in Fig. 2 for open and closed RCs to account for contributions by $\Delta E°(Q^-/Q)$. If only the radical pair standard free energy is considered there is a difference of 50 meV by which P^+I^- is elevated due to the presence of the negative charge on the neighboring Q. Furthermore, we have included in Fig. 2 the appropriate standard free energy changes resulting from the entropy term describing the delocalization of the exciton over all N antenna pigments. This N-fold degeneracy of the excited state decreases the standard free energy of the excited antenna relative to the radical pair state by $\Delta G = kt\,ln\,(1/N)$, equal to 112 meV under our conditions ($N = 80$, $T = 288°K$). The reference state with no such entropy contribution would be a hypothetical single antenna chlorophyll as shown in Fig. 2. The standard free energies of the radical pairs are presumably independent of the antenna size. Then, the effect by a large or small antenna

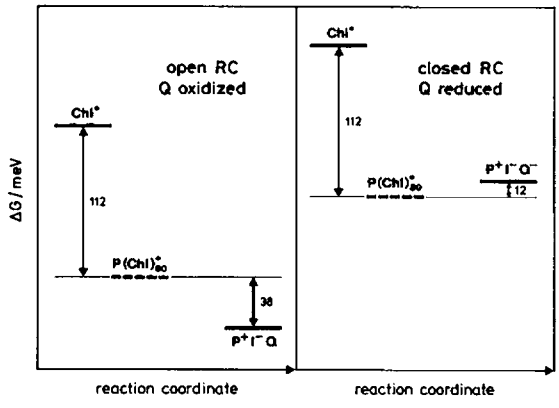

FIGURE 2 Scheme of standard free energy contents of excited and charge separated states involved in the primary processes in photosystem II particles and an antenna of ~80 Chl/P_{680}. The differences in ΔG between radical pairs and excited states are calculated from the data in Table II, those between the excited state of the PS II particles and the hypothetical single antenna Chl from the entropy change (see Discussion). The different levels of standard free energy of excited states in open and closed RCs account for the contributions by $n \cdot F \cdot \Delta E°(Q^-/Q)$.

on the standard free energy contents of $[P(Chl_N)]^*$ would involve a shift to lower or higher values, respectively, of the standard free energy.

It follows that a large antenna in vivo may serve several purposes. (*a*) It enables efficient photon absorption by a high optical cross-section. (*b*) It reduces the apparent rate constant of charge separation and acts as a temporary exciton storage system helping to match the intrinsically fast and reversible step of charge separation to the pace of the much slower subsequent charge stabilization. (*c*) It reduces the standard free energy change associated with charge separation, and hence allows for efficient charge separation at low intermediate concentrations of the primary radical pair P^+I^-. This may be the way nature has minimized the loss processes.

For the extreme case of an isolated PS II–RC devoid of antenna pigments a simple extrapolation predicts charge separation at a rate constant of $1/2.7$ ps^{-1}. This is in the time range of vibrational relaxation (see reference 35 and references therein). Thus, charge separation in the isolated RC occurs most likely from a nonequilibrium configuration in competition with vibrational relaxation (35, 39). This could be one reason for the much smaller decrease in the rate of charge separation upon closing the RC, which was observed by factors of 1.3 (30) to 1.6 (21) in isolated bacterial RCs as compared with a factor of ≥ 3 in chromatophores (40) or the factor of 6.2 in our PS II particles. The large standard free energy difference associated with charge separation in isolated RCs indicates also a high yield of radical pair formation. For the isolated RC of PS II one can expect from Fig. 2 a standard free energy difference between the excited and charge-separated states of ~150 meV. In isolated bacterial RCs the corresponding standard free energy gap has been determined to be 150 (41) or 160 meV (42).

The experimental observation (3) of slower fluorescence decay and reduced radical pair formation in PS II particles upon reduction of the primary quinone acceptor Q correlates within our model with a decrease of the rate of charge separation (Table II). The value of k_1 decreases by a factor of 6.2 when going from open to closed RCs. This decrease corresponds with an increase of the intrinsic time constants for charge separation from 2.7 to 16.7 ps. In contrast the rate constant for charge recombination k_2 is increased only to a very small extent upon reduction of Q. This finding appears surprising on a first glance. However, both the large decrease in k_1 as well as the very small increase in k_2 can be understood within a unified framework. In analogy to bacterial RCs we assume that in the case of open RCs the potential energy curves of the radical pair state P^+I^- and the excited state P* cross near the potential minimum of the latter state (43). This implies a basically activationless charge separation reaction for open RCs. The recombination reaction does require thermal activation, however. A schematic model depicting this situation is shown in Fig. 3. As we have discussed, for closed RCs the standard free

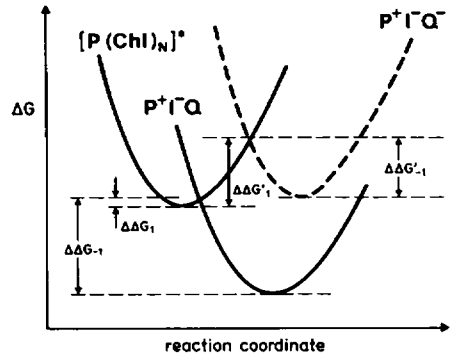

FIGURE 3 Schematic representation of the potential energy curves of the excited states and the radical pair states for oxidized (*solid line*) and reduced (*broken line*) quinone acceptor Q. The respective activation energies for the charge separation and charge recombination steps are also indicated in each case.

energy of the radical pair state is increased due to the interaction of P^+I^- with Q^-. Now the charge separation process is no longer activationless (see Fig. 3), resulting in a large decrease in the corresponding rate constant k_1. In contrast, the activation energy for the recombination process is expected to be changed only to a small extent, hence affecting the rate constant k_2 only to a small extent. Another reason for the large decrease in k_1 may be the change in vibrational wave-function overlap between P and I as discussed in reference 44. This could be equivalent to a drastic change in the Franck-Condon factor for the transition from P*I to P^+I^-.

The time dependences of the transient concentrations of each PS II component involved in the primary processes are shown in Fig. 4 on a dual time scale for PS II particles with $N = 80$ Chl/P_{680}. With open RCs initially there is a parallel rise of P^+ and I^-. Due to the onset of electron transfer from I^- to Q which starts after a short lag the I^- concentration passes through a maximum of 53% (relative to initially excited Chl*) after ~200 ps. The intermediate concentration maximum of I^- will be dependent on the antenna size as discussed above and in reference 5. After ~2.5 ns the charges are stabilized on P^+ and Q^- with a yield given by ${}^Pa_3$ (85% in our case). With closed RCs the consequences of the discussed rate changes are obvious from the comparison of the corresponding curves in Fig. 4. The transient concentration maximum of P^+I^- is now only ~23% and is reached at ~500 ps. A small portion, not detectable within the signal/noise ratio of measurements in reference 3, is converted into long-lived components, e.g., triplets or a relaxed radical pair state. As discussed above the effects exerted by an increased antenna size suggest that in unfractionated PS II the maximum of the intermediate radical pair concentration will be even lower.

A model assuming a fast energy transfer between all chlorophyll molecules in a photosynthetic unit and a high probability for multiple trapping and detrapping steps at the reaction center chlorophyll P, i.e., a shallow trap, was

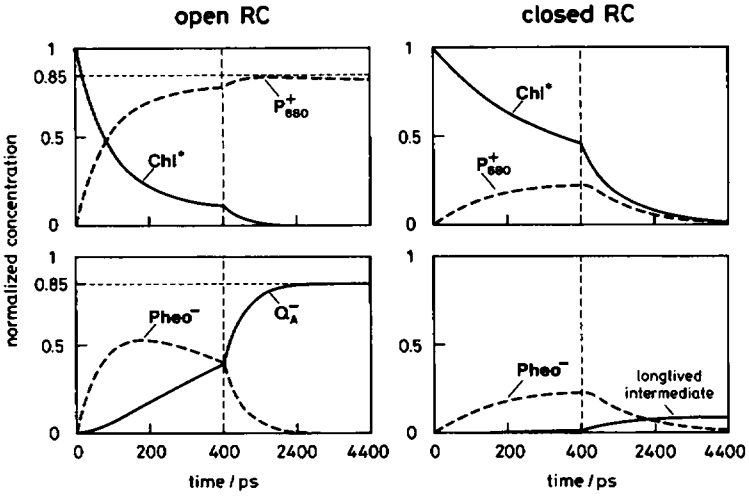

FIGURE 4 Schematic representation of the time-resolved normalized concentrations of each pigment component involved in the primary processes in photosystem II. Calculated for open (*left*) and closed (*right*) RCs according to Eq. A1 using the values from Table III. The time scale is compressed after 400 ps. The long-lived component(s) could be a triplet state and/or a relaxed radical pair state (see Discussion).

already proposed by Duysens (45). He estimated the rate of charge separation in PS II on the basis of relative chlorophyll fluorescence yields measured in chloroplasts with open and (partially) closed RCs (46). Notably, his results are very similar to ours, with time constants for charge separation of 2.5 ps in open and 14 ps in closed RCs, respectively.

CONCLUSIONS

We have presented a model of the photosynthetic RC of PS II and its associated Chl antenna which can explain the experimental picosecond kinetics of the primary processes. This model assumes that the intermolecular processes of single-step excitation transfer and charge separation proceed at rates faster than or comparable with vibrational relaxation occurring within a few picoseconds. The most striking result of the analysis consists in the conclusion, that the control of the radical pair yield is exerted primarily by the effect of the redox state of the quinone acceptor Q on the rate constant of the charge separation process. The charge recombination rate is affected to a much smaller extent. This result is in contrast to earlier interpretations and models which assumed that reduction of Q should result in an increased yield of transient radical pairs which would then give rise to charge recombination luminescence (1, 4).

Due to a tight coupling of N antenna pigments with the RC pigments the apparent rate of charge separation in vivo is shifted by a factor in the order of N to longer times as compared with an isolated reaction center. Thus, the system has enough time to reach thermal equilibrium. This very feature provides the basis for the apparent success of such simple models as shown in Fig. 1 and originally proposed in reference 5. Obviously, the use of principles of equilibrium thermodynamics allows to describe the energy partition between electronically excited and radical pair states. Such a collective model has the advantage over other models of requiring less detailed information on molecular parameters of the antenna organization and exciton interaction. Such information is still difficult or even impossible to determine experimentally.

The almost exact coincidence of the values discussed above for the rate of charge separation and the free energy differences in quite different RCs may perhaps be fortuitous given the simplifying assumptions made here and taking into account any measurement errors. Nevertheless, it indicates that the elementary intrinsic charge separation step in different photosynthetic RCs generally occurs within a few picoseconds. This step may be associated with standard free energy changes of similar magnitude in different types of RC.

APPENDIX

The differential rate equations of the states B, C, and D of the scheme in Fig. 1 were solved for the initial boundary condition $B(t = o) = 1$ using the Laplace transform method (47). The solutions are of the form

$$X(t) = \sum_i^3 x_i * \exp(-t/\tau_i) \tag{A1}$$

for each state X with three different lifetimes τ_i given by

$$1/\tau_1 = p + (p^2 - q^2)^{1/2} = -v \tag{A2}$$

$$1/\tau_2 = p - (p^2 - q^2)^{1/2} = -w \tag{A3}$$

$$1/\tau_3 = k_3, \tag{A4}$$

where

$$o = k_{-1} + k_2 \tag{A5}$$

$$p = \tfrac{1}{2}(k_A + k_1 + k_{-1} + k_2) \tag{A6}$$

$$q = (k_A k_{-1} + k_A k_2 + k_1 k_2)^{1/2}. \tag{A7}$$

Depending on the type of experiment only some of the states will be detected. Fluorescence exclusively monitors $B(t)$. Absorbance changes are expected by reactions involving Chl, P, and I only, because the absorbance changes by Z and Q in the red region of the spectrum are known to be small compared with those of the pigments (19). Thus, only three absorbance difference spectra remain to be considered.

$$\Delta\epsilon(\mathrm{Chl},\lambda) = \epsilon(\mathrm{Chl}^*) - \epsilon(\mathrm{Chl}) \quad \text{(A8)}$$

$$\Delta\epsilon(\mathrm{P},\lambda) = \epsilon(\mathrm{P}^+) - \epsilon(\mathrm{P}) \quad \text{(A9)}$$

$$\Delta\epsilon(\mathrm{I},\lambda) = \epsilon(\mathrm{I}^-) - \epsilon(\mathrm{I}). \quad \text{(A10)}$$

We now have to find the relationship between the lifetime-associated concentrations x_i, which are solutions of the Laplace transform, and the lifetime-associated amplitudes $A_i(\lambda)$ of absorbance changes, which are obtained as the result of the multiexponential analysis according to

$$A(\lambda,t) - A_o(\lambda) = \sum_i A_i(\lambda) * \exp(-t/\tau_i). \quad \text{(A11)}$$

These amplitudes are composed from the products of amplitude factors ${}^c a_i$ and the absorbance difference coefficients $\Delta\epsilon(c,\lambda)$ according to

$$A_i(\lambda) = \sum_c {}^c a_i * \Delta\epsilon(c,\lambda). \quad \text{(A12)}$$

Note: i is the lifetime index and c the component index. For each lifetime τ_i the amplitudes $A_i(\lambda)$ are then given by:

$$\begin{aligned} A_1(\lambda) = {}^{\mathrm{Chl}}a_1 * \Delta\epsilon(\mathrm{Chl},\lambda) + {}^{\mathrm{P}}a_1 * \Delta\epsilon(P,\lambda) \\ + {}^{\mathrm{I}}a_1 * \Delta\epsilon(\mathrm{I},\lambda) = \left(\frac{v+o}{v-w}\right) * \Delta\epsilon(\mathrm{Chl},\lambda) \\ + \left[\frac{k_1 v + k_1 k_3 + k_1 k_2}{(v-w)(v+k_3)}\right] * \Delta\epsilon(\mathrm{P},\lambda) \\ + \left(\frac{k_1}{v-w}\right) * \Delta\epsilon(\mathrm{I},\lambda) \end{aligned} \quad \text{(A13)}$$

$$\begin{aligned} A_2(\lambda) = {}^{\mathrm{Chl}}a_2 * \Delta\epsilon(\mathrm{Chl},\lambda) + {}^{\mathrm{P}}a_2 * \Delta\epsilon(\mathrm{P},\lambda) \\ + {}^{\mathrm{I}}a_2 * \Delta\epsilon(\mathrm{I},\lambda) = \left(\frac{w+o}{w-v}\right) * \Delta\epsilon(\mathrm{Chl},\lambda) \\ + \left[\frac{k_1 k_3 + k_1 w + k_1 k_2}{(w-v)(k_3+w)}\right] * \Delta\epsilon(\mathrm{P},\lambda) \\ + \left(\frac{k_1}{w-v}\right) * \Delta\epsilon(\mathrm{I},\lambda) \end{aligned} \quad \text{(A14)}$$

$$\begin{aligned} A_3(\lambda) = {}^{\mathrm{P}}a_3 * \Delta\epsilon(\mathrm{P},\lambda) \\ = \left[\frac{k_1 k_2}{(v+k_3)(k_3+w)}\right] * \Delta\epsilon(\mathrm{P},\lambda). \end{aligned} \quad \text{(A15)}$$

We thank Prof. K. Schaffner for his interest in this work.

Partial financial support by the Deutsche Forschungsgemeinschaft is acknowledged.

Received for publication 28 December 1987 and in final form 4 May 1988.

REFERENCES

1. Klimov, V. V., and A. A. Krasnovskii. 1982. Participation of pheophytin in the primary processes of electron transfer at the reaction centers of photosystem II. *Biophysics (Engl. Transl. Biofizika)*. 27:186–198.
2. Nuijs, A. M., H. J. van Gorkom, J. J. Plijter, and L. N. M. Duysens. 1986. Primary-charge separation and excitation of chlorophyll *a* in photosystem II particles from spinach as studied by picosecond absorbance-difference spectroscopy. *Biochim. Biophys. Acta.* 848:167–175.
3. Schatz, G. H., H. Brock, and A. R. Holzwarth. 1987. Picosecond kinetics of fluorescence and of absorbance changes in photosystem II particles excited at low photon density. *Proc. Natl. Acad. Sci. USA.* 84:8414–8418.
4. Shuvalov, V. A., V. V. Klimov, E. Dolan, W. W. Parson, and B. Ke. 1980. Nanosecond fluorescence and absorbance changes in photosystem II at low redox potential. *FEBS (Fed. Eur. Biochem. Soc.) Lett.* 118:279–282.
5. Schatz, G. H., and A. R. Holzwarth. 1986. Mechanisms of chlorophyll fluorescence revisited: prompt or delayed emission from photosystem II with closed reaction centers? *Photosynth. Res.* 10:309–318.
6. Trissl, H.-W., J. Breton, J. Deprez, and W. Leibl. 1987. Primary electrogenic reactions of photosystem II as probed by the light-gradient method. *Biochim. Biophys. Acta.* 893:305–319.
7. Holzwarth, A. R., H. Brock, and G. H. Schatz. 1987. Picosecond transient absorbance spectra and fluorescence decay kinetics in photosystem II particles. *In* Progress in Photosynthesis Research. Vol. 1. J. Biggins, editor. Martinus Nijhoff Publishers, Dordrecht, The Netherlands. 61–65.
8. Pearlstein, R. M., 1982. Chlorophyll singlet excitons. *In* Photosynthesis: Energy Conversion by Plants and Bacteria. Vol. 1. Govindjee, editor. Academic Press, New York. 293–330.
9. van Grondelle, R. 1985. Excitation energy transfer, trapping and annihilation in photosynthetic systems. *Biochim. Biophys. Acta.* 811:147–195.
10. Thielen, A. P. G. M., and H. J. van Gorkom. 1981. Energy transfer and quantum yield in photosystem II. *Biochim. Biophys. Acta.* 637:439–446.
11. Kramer, H., and P. Mathis. 1980. Quantum yield and rate of formation of the carotenoid triplet state in photosynthetic structures. *Biochim. Biophys. Acta.* 593:319–329.
12. Kura-Hotta, M., K. Satoh, and S. Katoh. 1986. Functional linkage between phycobilisome and reaction center in two phycobilisome oxygen-evolving photosystem II preparations isolated from the thermophilic cyanobacterium *Synechococcus sp. Arch. Biochem. Biophys.* 249:1–7.
13. den Blanken, H. J., A. J. Hoff, A. P. J. M. Jongenelis, and B. A. Diner. 1983. High-resolution triplet-minus-singlet absorbance difference spectrum of photosystem II particles. *FEBS (Fed. Eur. Biochem. Soc.) Lett.* 157:21–27.
14. Takahashi, Y., O. Hansson, P. Mathis, and K. Satoh. 1987. Primary radical pair in the photosystem II reaction center. *Biochim. Biophys. Acta.* 893:49–59.
15. Nordlund, T. M., and W. H. Knox. 1981. Lifetime of fluorescence from light-harvesting chlorophyll *a/b* proteins. Excitation intensity dependence. *Biophys. J.* 36:193–201.
16. Il'ina, M. D., E. A. Kotova, and A. Y. Borisov. 1981. The detergent and salt effect on the light-harvesting chlorophyll *a/b* complex from green plants. *Biochim. Biophys. Acta.* 636:193–200.
17. Ide, J. P., D. R. Klug, W. Kühlbrandt, G. Porter, and J. Barber. 1986. Detergent effects upon the picosecond dynamics of higher plant light harvesting chlorophyll complex (LHC). *In* Ultrafast Phenomena V. G. R. Fleming and A. E. Siegman, editors. Springer-Verlag, Berlin. 406–408.
18. Pearlstein, R. M. 1984. Photosynthetic exciton migration and trapping. *In* Advances in Photosynthesis Research. Vol. 1. C. Sybesma, editor. Martinus Nijhoff, The Hague. 13–20.
19. Schatz, G. H., and H. J. van Gorkom. 1985. Absorbance difference spectra upon charge transfer to secondary donors and acceptors in photosystem II. *Biochim. Biophys. Acta.* 810:283–294.
20. Martin, J.-L., J. Breton, A. J. Hoff, A. Migus, and A. Antonetti. 1986. Femtosecond spectroscopy of electron transfer in the reaction center of the photosynthetic bacterium *Rhodopseudomonas sphaeroides* R-26. Direct electron transfer from the dimeric

bacteriochlorophyll primary donor to the bacteriopheophytin acceptor with a time constant 2.8 +/− 0.2 psec. *Proc. Natl. Acad. Sci. USA.* 83:957–961.

21. Breton, J., J.-L. Martin, A. Migus, A. Antonetti, and A. Orszag. 1986. Femtosecond spectroscopy of excitation energy transfer and initial charge separation in the reaction center of the photosynthetic bacterium *Rhodopseudomonas sphaeroides. In* Ultrafast Phenomena V. G. R. Fleming and A. E. Siegman, editors. Springer-Verlag, Berlin. 393–397.
22. Breton, J., J.-L. Martin, A. Migus, A. Antonetti, and A. Orszag. 1986. Femtosecond spectroscopy of excitation energy transfer and initial charge separation in the reaction center of the photosynthetic bacterium *Rhodopseudomonas viridis. Proc. Natl. Acad. Sci. USA.* 83:5121–5125.
23. Zinth, W., J. Dobler, and W. Kaiser. 1986. Femtosecond spectroscopy of the primary events of bacterial photosynthesis. *In* Ultrafast Phenomena V. G. R. Fleming and A. E. Siegman, editors. Springer-Verlag, Berlin. 379–383.
24. Robinson, G. W. 1967. Excitation transfer and trapping in photosynthesis. *Brookhaven Symp. Biol.* 19:16–48.
25. Owens, T. G., S. P. Webb, L. Mets, R. S. Alberte, and G. R. Fleming. 1987. Antenna size dependence of fluorescence decay in the core antenna of photosystem I: estimates of charge separation and energy transfer rates. *Proc. Natl. Acad. Sci. USA.* 84:1532–1536.
26. Pearlstein, R. M. 1982. Exciton migration and trapping in photosynthesis. *Photochem. Photobiol.* 35:835–844.
27. Melis, A., and J. M. Anderson. 1983. Structural and functional organization of the photosystems in spinach chloroplasts. Antenna size, relative electron-transport capacity, and chlorophyll composition. *Biochim. Biophys. Acta.* 724:473–484.
28. Holzwarth, A. R., J. Wendler, and W. Haehnel. 1985. Time-resolved picosecond fluorescence spectra of the antenna chlorophylls in *Chlorella vulgaris.* Resolution of Photosystem I fluorescence. *Biochim. Biophys. Acta.* 807:155–167.
29. Schatz, G. H., and A. R. Holzwarth. 1987. Picosecond time resolved chlorophyll fluorescence spectra from pea chloroplast thylakoids. *In* Progress in Photosynthesis Research. Vol. 1. J. Biggins, editor. Martinus Nijhoff Publishers, Dordrecht, The Netherlands. 67–69.
30. Woodbury, N. W., M. Becker, D. Middendorf, and W. W. Parson. 1985. Picosecond kinetics of the initial photochemical electron-transfer reaction in bacterial photosynthetic reaction centers. *Biochemistry.* 24:7516–7521.
31. Sebban, P., and I. Moya. 1983. Fluorescence lifetime spectra of in vivo bacteriochlorophyll at room temperature. *Biochim. Biophys. Acta.* 722:436–442.
32. Sebban, P., G. Jolchine, and I. Moya. 1984. Spectra of fluorescence lifetime and intensity of *Rhodopseudomonas sphaeroides* at room and low temperature. Comparison between the wild type, the c_{71} reaction center-less mutant and the B800–850 pigment-protein complex. *Photochem. Photobiol.* 39:247–253.
33. Borisov, A. Y., A. M. Freiberg, V. I. Godik, K. K. Rebane, and K. E. Timpmann. 1985. Kinetics of picosecond bacteriochlorophyll luminescence in vivo as a function of the reaction center state. *Biochim. Biophys. Acta.* 807:221–229.
34. Shipman, L. L., and D. L. Housman. 1979. Förster transfer rates for chlorophyll a*. *Photochem. Photobiol.* 29:1163–1167.
35. Jortner, J. 1980. Dynamics of the primary events in bacterial photosynthesis. *J. Am. Chem. Soc.* 102:6676–6686.
36. Nedbal, L., and V. Szocs. 1986. How long does excitonic motion in the photosynthetic unit remain coherent? *J. Theor. Biol.* 120:411–418.
37. Junge, W., and J. B. Jackson. 1982. The development of electrochemical potential gradients across photosynthetic membranes. *In* Photosynthesis: Energy Conversion by Plants and Bacteria. Vol. 1. Govindjee, editor. Academic Press, New York. 589–646.
38. Deisenhofer, J., O. Epp, K. Miki, R. Huber, and H. Michel. 1984. X-ray structure-analysis of a membrane-protein complex. Electron density map at 3A resolution and a model of the chromophores of the photosynthetic reaction center from *Rhodopseudomonas viridis. J. Mol. Biol.* 180:385–398.
39. Friesner, R., and R. Wertheimer. 1982. Model for primary charge separation in reaction centers of photosynthetic bacteria. *Proc. Natl. Acad. Sci. USA.* 79:2138–2142.
40. Vos, M., R. van Grondelle, F. W. van der Kooij, D. van de Poll, J. Amesz, and L. N. M. Duysens. 1986. Singlet-singlet annihilation at low temperatures in the antenna of purple bacteria. *Biochim. Biophys. Acta.* 850:501–512.
41. van Grondelle, R., N. G. Holmes, H. Rademaker, and L. N. M. Duysens. 1978. Bacteriochlorophyll fluorescence of purple bacteria at low redox potentials. Relationship between reaction center triplet yield and the emission yield. *Biochim. Biophys. Acta.* 503:10–25.
42. Woodbury, N. W. T., and W. W. Parson. 1984. Nanosecond fluorescence from isolated photosynthetic reaction centers of *Rhodopseudomonas sphaeroides. Biochim. Biophys. Acta.* 767:345–361.
43. Marcus, R. A., and N. Sutin. 1985. Electron transfer in chemistry and biology. *Biochim. Biophys. Acta.* 811:265–322.
44. Devault, D. 1986. Vibronic coupling to electron transfer and the structure of the *Rhodopseudomonas viridis* reaction center. *Photosynth. Res.* 10:125–137.
45. Duysens, L. N. M. 1979. Transfer and trapping of excitation energy in photosystem II. *In* Chlorophyll Organization and Energy Transfer in Photosynthesis. *CIBA Found. Symp.* 61:323–340.
46. van Gorkom, H. J., M. P. J. Pulles, and A.-L. Etienne. 1978. Fluorescence and absorbance changes in tris-washed chloroplasts. *In* Photosynthetic Oxygen Evolution. H. Metzner, editor. Academic Press, London. 135–145.
47. Oberhettinger, F., and L. Badii. 1973. Tables of Laplace Transforms. Springer-Verlag, Berlin. 427 pp.